PCP
PLANT & CELL PHYSIOLOGY

Regular Paper

Phosphatidylserine Synthase from *Salicornia europaea* Is Involved in Plant Salt Tolerance by Regulating Plasma Membrane Stability

Sulian Lv[1,5], Fang Tai[1,2,5], Jie Guo[1,3], Ping Jiang[1], Kangqi Lin[1,4], Duoliya Wang[1,4], Xuan Zhang[1,4] and Yinxin Li[1,*]

[1]Key Laboratory of Plant Molecular Physiology, Institute of Botany, Chinese Academy of Sciences, Beijing 100093, China
[2]Laboratory of Genetics and Breeding of Marine Organism, College of Marine Life Sciences, Ocean University of China, Qingdao 266003, China
[3]Linda Liu and Partners, Beijing 100000, China
[4]College of Life Sciences, University of Chinese Academy of Sciences, Beijing 100049, China
[5]The first two authors contributed equally to this work
*Corresponding author: E-mail, yxli@ibcas.ac.cn; Fax, +86 10 62836691.
(Received 26 March 2020; Accepted 24 October 2020)

Salinity-induced lipid alterations have been reported in many plant species; however, how lipid biosynthesis and metabolism are regulated and how lipids work in plant salt tolerance are much less studied. Here, a constitutively much higher phosphatidylserine (PS) content in the plasma membrane (PM) was found in the euhalophyte *Salicornia europaea* than in Arabidopsis. A gene encoding PS synthase (PSS) was subsequently isolated from *S. europaea*, named *SePSS*, which was induced by salinity. Multiple alignments and phylogenetic analysis suggested that SePSS belongs to a base exchange-type PSS, which localises to the endoplasmic reticulum. Knockdown of *SePSS* in *S. europaea* suspension cells resulted in reduced PS content, decreased cell survival rate, and increased PM depolarization and K^+ efflux under 400 or 800 mM NaCl. By contrast, the upregulation of *SePSS* leads to increased PS and phosphatidylethanolamine levels and enhanced salt tolerance in Arabidopsis, along with a lower accumulation of reactive oxygen species, less membrane injury, less PM depolarization and higher K^+/Na^+ in the transgenic lines than in wild-type (WT). These results suggest a positive correlation between PS levels and plant salt tolerance, and that SePSS participates in plant salt tolerance by regulating PS levels, hence PM potential and permeability, which help maintain ion homeostasis. Our work provides a potential strategy for improving plant growth under multiple stresses.

Keywords: Depolarization • Membrane permeability • Phosphatidylserine • Plasma membrane • *Salicornia europaea* L • Salt tolerance.

Accession numbers: The nucleotide sequence reported in this article has been submitted to GenBank under the accession number **KF501401**.

Introduction

Soil salinization is one of the major environmental factors threatening crop productivity worldwide. The injurious effects of salinity on plants are associated with three main elements: ion imbalance, which can cause nutrient stress; osmotic stress, which affects the uptake of water; and oxidative stress due to the generation of reactive oxygen species (ROS). As the selective barrier dividing living cells from their environments, the plasma membrane (PM) might be the primary site of salt injury, which is integral to all these components of salt stress. The PM potential, permeability, activities of membrane-bound enzymes and lipid composition can be affected in plant response to salt stress (Mansour 2013, Guo et al. 2019). Maintaining PM stability and integrity under salinity is one of the important salt adaptation strategies in many salt-tolerant plants (Mansour 2013).

The plant membrane potential reports on the activity of electrogenic PM transport processes. Three dominant membrane potential states can be distinguished: resting, hyperpolarized and depolarized (Roelfsema et al. 2001). Generally, in the resting state, the cell membrane maintains a polarity with internal electronegative, which is dominated by the proton pumps such as H^+-ATPase and ion channels in PM (Konrad and Hedrich 2008). Upon salt stress, Na^+ enters into the cell via nonselective cation channels leading to PM depolarization, which results in cytosolic K^+ efflux regulated by depolarization-activated outward rectifying K^+ channels (DA-KORCs) and depolarization-activated nonselective cation channels (DA-NSCCs) (Chen et al. 2005). Salt-resistant species possess a strong ability to maintain the membrane potential and thus K^+/Na^+ homeostasis under salinity (Zhu 2003).

Phospholipids are essential components of cellular membranes and signal transduction cascades in plants (Nakamura 2017). With two hydrophobic fatty acyl groups and a

Plant Cell Physiol. 62(1): 66–79 (2021) doi:10.1093/pcp/pcaa141, Advance Access publication on 3 November 2020, available online at https://academic.oup.com/pcp

hydrophilic polar head group attached to the glycerol backbone, phospholipids are asymmetrically distributed in the cell membrane. According to their molecular structure, phospholipids can be divided into bilayer-forming lipids, including phosphatidylcholine (PC), phosphatidic acid (PA), phosphatidylinositol (PI), phosphatidylserine (PS), phosphatidylglycerol (PG) and non-bilayer lipids, such as phosphatidylethanolamine (PE). As the dominant membrane phospholipids, PC and PE have been extensively studied (reviewed in Guo et al. 2019). Many studies have shown alterations in phospholipid amount and species in plants subjected to salt stress, which suggest a positive correlation between phospholipid content and plant salt tolerance (Salama et al. 2007, Alvarez-Pizarro et al. 2009). Although less abundant than PC and PE in the membrane, evidence has shown that the negatively charged PI and PS are crucial for plant salt tolerance. Increased PI and PS were found in roots of salt-tolerant buffalo grass, callus of the halophyte *Spartina patens* and root PM of salt-treated wheat (Lin and Wu 1996, Wu et al. 2005, Salama and Mansour 2015). However, the function mechanism of PI and PS in plant salt tolerance remains unclear, although it is assumed that the higher amounts of negatively charged PI and PS would result in a higher PM affinity for Ca^{2+} of PM (Lin and Wu 1996).

In contrast to other anionic phospholipids, PS is relatively abundant, representing as much as 10–20% of the total phospholipids at the PM inner leaflet (Leventis and Grinstein 2010). PS plays an important role in cell death signaling, vesicular trafficking, lipid–protein interactions and membrane lipid metabolism (Vance 2008). The biosynthesis pathway of PS varies in different species. In bacteria and yeast, PS is synthesized by a PS synthase (CD-PSS) that utilizes CDP-diacylglycerol and L-serine (Ser) as substrates (Matsumoto 1997). In mammals, PS is synthesized by a calcium-dependent base exchange-type PSS (BE-PSS) with PE or PC as a substrate. Interestingly, both pathways have been reported in different plant species. The CD-PSS activity was found in spinach (Marshall and Kates 1974) and wheat (Delhaize et al. 1999), whereas BE-PSS was found in Arabidopsis (Yamaoka et al. 2011) and rice (Yin et al. 2013, Rani et al. 2020). In Arabidopsis, *PSS1*, the single gene encoding BE-PSS, was found essential for microspore, inflorescence meristem and organ development (Yamaoka et al. 2011, Liu et al. 2013). Similarly, *OsPSS* was found to regulate stem development and control cell elongation by regulating exocytosis in rice (Yin et al. 2013, Ma et al. 2016). Very recently, an *ES5* encoding PSS was reported to be involved in leaf senescence by regulating PS levels in rice (Rani et al. 2020). Till now, there have been no studies that investigate PSS roles in plant response to salinity.

Salicornia europaea L., a succulent euhalophyte in Chenopodiaceae, is widely distributed in coastal and inland salt marshes. *Salicornia europaea* plants showed optimal growth under 200–400 mM NaCl (Lv et al. 2012). It can withstand >1000 mM NaCl and is one of the most salt-tolerant plant species in the world (Flowers and Colmer 2008, Wang et al. 2009). In this study, we first found that *S. europaea* had a constitutively much higher PS content in PM of the shoot than Arabidopsis under either non-salt or salt conditions. To further evaluate the potential role that PS could play in plant salt tolerance, we subsequently isolated a gene encoding PSS from *S. europaea* and investigated its function by gene knocking down in *S. europaea* suspension cells and overexpression in Arabidopsis. The results indicated that SePSS was involved in plant salt tolerance by regulating PS and PE levels, hence PM stability, which help maintain K^+/Na^+ homeostasis under salinity. Based on our results and the previous studies, several potential roles of PS involved in plant salt tolerance were postulated.

Results

PS in PM increased under salinity and *S. europaea* showed constitutively higher PS content than Arabidopsis

To investigate the response of PS to salt stress, the total PS content in PM of *S. europaea* shoots and Arabidopsis leaves under different NaCl concentrations was measured. In general, PS content in PM increased with the increase in NaCl concentration in both species (**Fig. 1a**). Interestingly, in *S. europaea*, PS increased up to 3.3-fold under 800 mM NaCl, while the value is 15.7-fold in Arabidopsis under 200 mM NaCl (**Fig. 1a**). This difference was mainly due to the much lower PS levels in Arabidopsis under the non-salt condition. The total amount of PS in *S. europaea* was about 18.5-fold of that in Arabidopsis under the non-salt condition. Furthermore, PS levels in *S. europaea* were also significantly higher than that in Arabidopsis under all NaCl treatments.

As for the percentage of PS in the total PM lipids, it was also significantly higher in *S. europaea* than that in Arabidopsis either under non-salt or salt conditions (**Fig. 1b**). Under non-salt conditions, PS comprised 1.55% of total PM lipids in *S. europaea*, while it was only 0.36% in Arabidopsis. Under NaCl treatments, the percentage of PS increased to 0.53–0.80% in Arabidopsis, while it was maintained 1.18–2.16% in *S. europaea* (**Fig. 1b**).

SePSS encodes a PSS that localises to the endoplasmic reticulum

We identified one *PSS* transcript in the transcriptome analysis in *S. europaea* under salinity (Fan et al. 2013). The full length of *PSS* cDNA (GenBank accession no. KF501401) was then cloned from *S. europaea*, which encodes a protein of 419 amino acids. Multiple alignments showed that SePSS shares 70 and 78% identity with AtPSS1 from Arabidopsis and EsPSS1 from *Eutrema salsugineum*, respectively. As shown in **Supplementary Fig. S1a**, SePSS contains the residues responsible for CgPSS1 catalytic activity, free Ser binding/recognition, PSS1 regulation and PSS production and/or stability (Ohsawa et al. 2004). Phylogenetic tree analysis indicated that SePSS, EsPSS1 and AtPSS1were closely related (**Supplementary Fig. S1b**). SePSS contains seven transmembrane domains, as predicted by TMHMM Server 2.0 (**Supplementary Fig. S1c**).

The localization of SePSS was next studied by confocal microscopy. When SePSS-GFP and HDEL-mCherry were co-expressed in *Nicotiana benthamiana* cells, the overlapped signals of GFP and mCherry could be clearly viewed

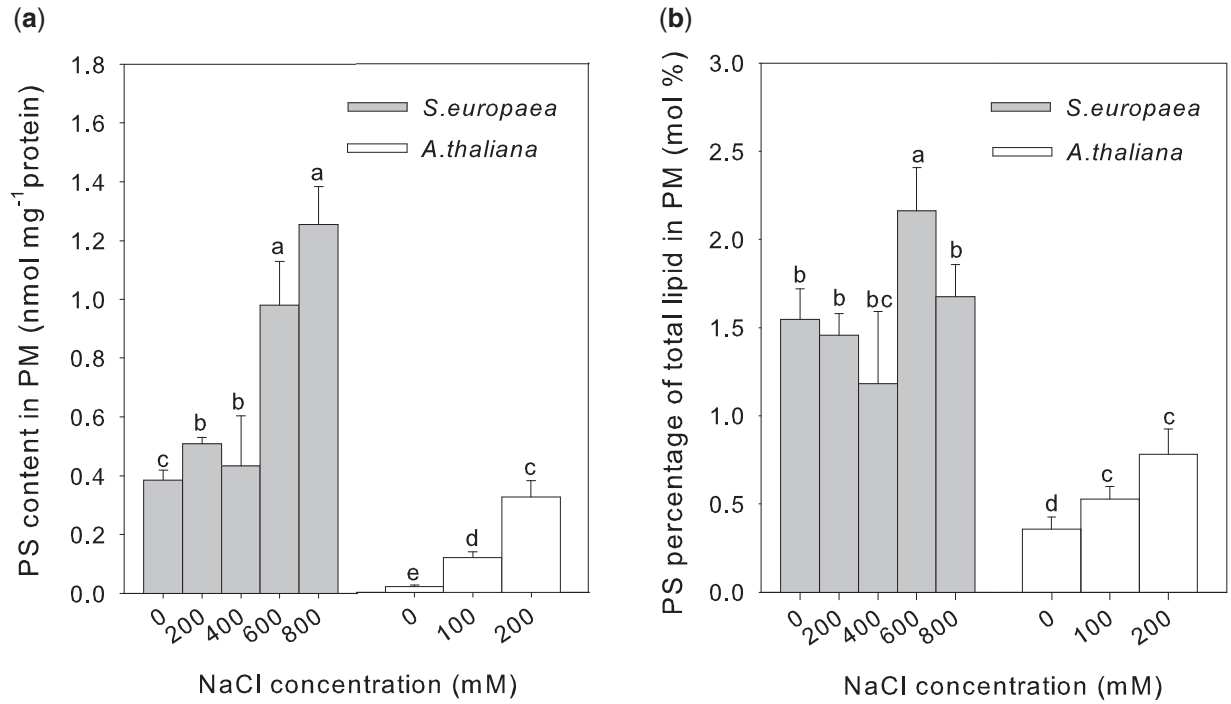

Fig. 1 PS content and percentage in PM of *S. europaea* shoots and Arabidopsis leaves under different NaCl concentrations. (a) Total PS content in PM and (b) PS percentage of total lipids in PM. For PS measurement, 21-day-old *S. europaea* and Arabidopsis plants were treated with the indicated NaCl concentrations for 2 weeks after which the shoot or leaf PM was isolated. PM lipid samples were analyzed by electrospray Ionization tandom mass spectrometry (ESI-MS/MS). Values are mean ± SE ($n = 5$). Different letters above the bars indicate significant differences at $P < 0.05$.

(**Supplementary Fig. S1d**). The results clearly confirmed the presence of SePSS in endoplasmic reticulum (ER) membranes.

SePSS was induced by salt treatment

To investigate the roles of SePSS in *S. europaea* response to salinity, gene expression profiles were analyzed. As shown in **Fig. 2**, *SePSS* was upregulated during 200 or 800 mM NaCl treatment, with the peak of expression being detected at 12 h. In contrast to 200 mM NaCl, 800 mM NaCl treatment induced gene expression more significantly. In plants exposed to 200 and 800 mM NaCl for 12 h, the transcript abundance of *SePSS* increased to about 5- and 13-fold of the control, respectively.

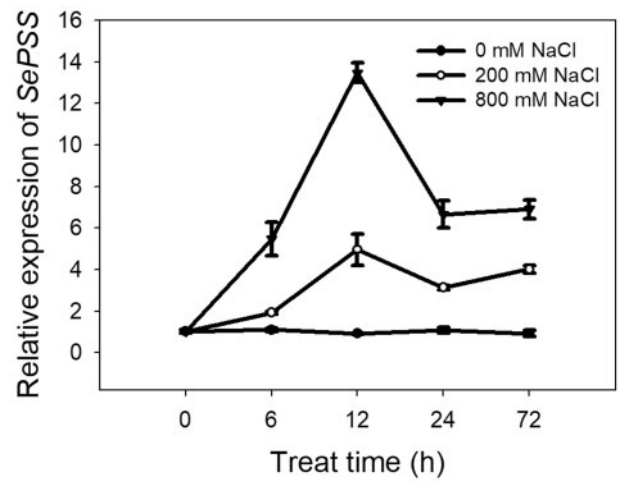

Fig. 2 Expression patterns of *SePSS* under different NaCl concentrations. One-month-old seedlings were treated with 1/2 Hoagland's solution containing 0, 200 or 800 mM NaCl. Shoots from at least three plants under each treatment were sampled at 0, 6, 12, 24 and 72 h. The *α-tubulin* gene from *S. europaea* was used as an internal control. Vertical bars indicate ± SE of three replicates on one sample. Three biological experiments were performed, which produced similar results.

Knockdown of *SePSS* in *S. europaea* cells resulted in decreased salt tolerance

To better understand the roles of SePSS in *S. europaea*, we established suspension-cultured cells reducing the *SePSS* transcript level by means of RNA interference (RNAi) (**Fig. 3a**). In RNAi lines, the amount of *SePSS* transcript decreased to only 3% of that in the empty vector (EV) cells (**Fig. 3b**). And PS content in the PM of RNAi callus showed about a 15% reduction compared with EV ones (**Fig. 3c**).

Cell viability of EV and RNAi lines under different concentrations of NaCl was first determined by fluorescein diacetate (FDA)–propidium iodide (PI) staining method to study the salt tolerance of these cells. Viable cells stained by FDA fluoresced bright green, while dead or dying cells stained by PI were bright red (**Fig. 3d**). As shown in **Fig. 3e**, the percentage of viable cells in RNAi cells was significantly lower than that of EV ones under all treatment conditions. Treatment of 400 mM NaCl for 8 h had no obvious effect on EV cells, while the survival percentages of RNAi line were significantly decreased to 59.7% from the control conditions (82.7%). Under 800 mM NaCl, the survival of EV and RNAi cells was 83.9 and 45.2%, respectively. These results indicated that the knockdown of *SePSS* enhanced the salt sensitivity of *S. europaea* cells.

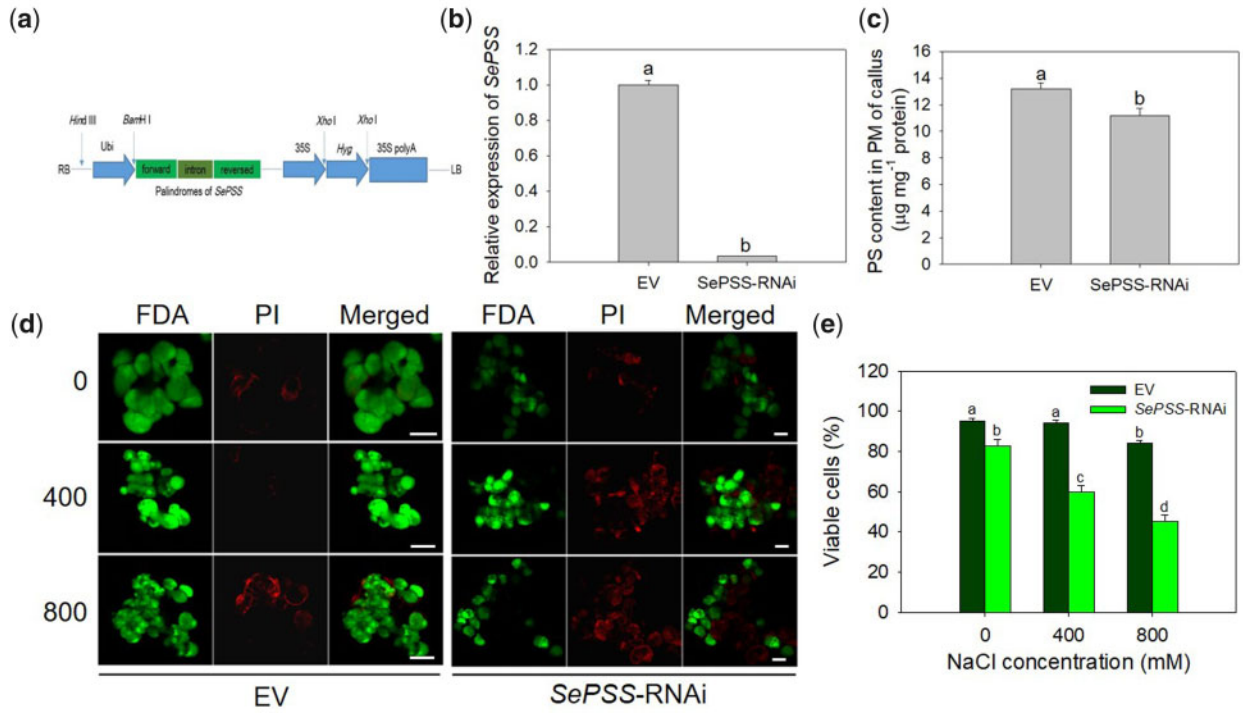

Fig. 3 Knockdown of *SePSS* in *S. europaea* cells led to decreased cell viability under salinity. (a) Schematic representation of transforming construct pU1301-*SePSS*-RNAi, (b) relative expression of *SePSS* in EV control and RNAi cells and (c) PS content in PM of EV and RNAi cells. (d) Confocal images of cells stained by FDA and PI simultaneously. Viable cells stained by FDA fluoresced bright green, while dead or dying cells stained by PI were bright red. Scale bars = 50 μm. (e) Percentage of viable cells. Suspension-cultured cells from the EV control and *SePSS*-RNAi lines were treated with NaCl (0, 400 and 800 mM) for 8 h and stained with 5 μM FDA and 10 μM PI in the dark for 40 min. Values are mean ± SE [$n = 3$ for (b), $n = 6$ for (c) and $n = 10$ for (e)]. Different letters above the bars indicate significant differences at $P < 0.05$.

SePSS regulated PM depolarization and K^+ flux under salt treatment

PM depolarization often occurs in plants subjected to salt stress, which leads to the leakage of K^+ from the cell (Nocito et al. 2002, Shabala et al. 2005). To investigate the possible role of SePSS in regulating membrane potential under salinity, EV and *SePSS*-RNAi cells were treated with 0, 400 and 800 mM NaCl and changes in the PM depolarization were monitored by using bis-(1,3-dibutylbarbituric acid)-trimethine oxonol (DiBAC4(3)). As shown in **Fig. 4a, b**, in EV cells, DiBAC4(3)-dependent fluorescence could be observed only under 800 mM NaCl, showing a PM depolarized. However, *SePSS*-RNAi cells showed higher fluorescence signals than EV cells under all the treatments, indicating a more pronounced PM depolarization.

Net K^+ fluxes were further detected using Non-invasive Micro-test Technology (NMT). Compared to the non-salt treatment, 400 and 800 mM NaCl treatment caused a decrease in K^+ influx in EV cells, while 800 mM NaCl treatment caused a shift of K^+ influx toward an efflux in *SePSS*-RNAi cells (**Fig. 4c**). These results imply that knockdown of *SePSS* may exacerbate NaCl-induced PM depolarization, which leads to the leakage of K^+ from the cell.

Overexpression of *SePSS* increased PS and PE in the PM of Arabidopsis

To better understand the role of SePSS in plant salt tolerance, *SePSS* was overexpressed in Arabidopsis and three transgenic lines OE2, 7 and 9 were analyzed. Considering the conversion between PS, PE and PC and the common substrate phosphoethanolamine (PEtn) used in PE and PC syntheses (Nakamura 2017), PS, PE and PC levels in PM were determined in wild-type (WT), EV and transgenic Arabidopsis. The results showed that there was no significant difference in PS, PE and PC levels between WT and EV plants (**Fig. 5**). As expected, PS in PM in transgenic lines increased significantly, which were 2.0–2.4 folds of that in WT plants (**Fig. 5a**). It is interesting to note that the PE levels were also higher in the transgenic lines than in WT and EV plants (**Fig. 5b**). The increased PE may be from the increased PS catalyzed by PSD, which has three isozymes in Arabidopsis, namely, PSD1, PSD2 and PSD3 (Nerlich et al. 2007). Results of gene expression analysis by quantitative real-time PCR (qRT-PCR) further confirmed this inference, which indicated the great upregulation of the three genes encoding PSD isozymes in the transgenic lines (**Supplementary Fig. S3**). PC content showed no obvious differences between transgenic lines and WT (**Fig. 5c**).

Overexpression of *SePSS* conferred less membrane injury and higher salt tolerance in Arabidopsis

Grown in 1/2 MS medium containing 1% (w/v) sucrose (CK), the transgenic seedlings showed no obvious difference with WT. However, seedlings from all transgenic lines outperformed WT under salt stress (**Fig. 6a**). The fresh weight (FW) of transgenic seedlings was significantly higher than that of WT, with an

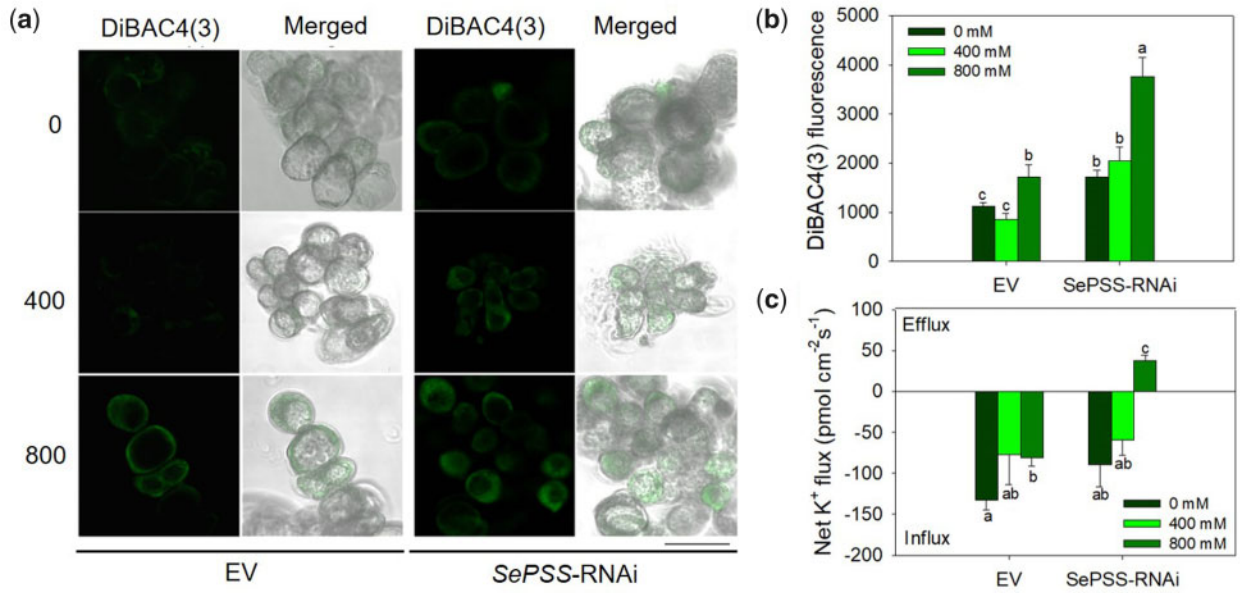

Fig. 4 PM depolarization and net K^+ fluxes in *S. europaea* cells under different NaCl concentrations. (a) Confocal images of cells stained by DiBAC4(3). Scale bars = 50 μm. (b) Relative DiBAC4(3) fluorescence. *Salicornia europaea* suspension cells of *SePSS*-RNAi and the EV controls were incubated in the dark for 15 min with 1 μM DiBAC4(3) in a medium containing 0, 400 and 800 mM NaCl. Cells from at least 10 microscope fields under 20× objective were analyzed. Values are mean ± SE ($n = 12$). (c) Net K^+ fluxes in *S. europaea* cells assayed by the NMT system. K^+ fluxes of *S. europaea* suspension cells of *SePSS*-RNAi and the EV controls were detected in the measuring solution after 2 h treatment under 0, 400 and 800 mM NaCl. The K^+ fluxes of the sample cells were recorded for 5 min. Values are mean ± SE ($n = 3$). Different letters above the bars indicate significant differences at $P < 0.05$.

increase of 26–37% and 25–41% under 100 and 150 mM NaCl, respectively (**Fig. 6c**). Higher chlorophyll content was also detected in the transgenic plants under 150 mM NaCl (**Fig. 6d**). However, the primary root length showed no significant difference between the transgenic lines and WT regardless of the growth medium (**Supplementary Fig. S3**).

The enhanced tolerance to salt stress in *SePSS*-overexpressing plants was further confirmed when 21-day-old plants grown in soil were subjected to 150 mM NaCl. After 14 d of salt treatment, most WT plants withered and the leaves became chlorotic, whereas the transgenic plants were slightly affected (**Fig. 6b**). Malondialdehyde (MDA, a product of membrane lipid peroxidation) accumulation and membrane ion leakage have been widely used to estimate the cell membrane stability under salinity. Consistently, the transgenic plants showed lower MDA levels and membrane ion leakage than WT (**Fig. 6e, f**), which suggested that less membrane injury occurs in transgenic plants under salt stress (Dionisio-Sese and Tobita 1998).

Salt stress can accelerate the production of ROS, which can result in oxidative stress and cause oxidative damage to nucleic acids, lipids and proteins, and the ability of plants to control ROS levels is highly correlated with its stress tolerance (Apel and Hirt 2004, Cheeseman 2007). Therefore, H_2O_2 and ROS levels were compared between WT and transgenic lines under salt stress. As shown in **Fig. 6g**, H_2O_2 content in leaves increased under salt stress in both transgenic and WT plants, among which the increase in WT was the largest. Under salt stress, transgenic lines showed 32–37% lower H_2O_2 levels than WT. Consistent with these results, increased ROS accumulation was observed by 2′,7′dichlorofluorescin diacetate (H_2DCFDA) fluorescence with the NaCl concentration, and the fluorescence intensity was significantly lower in OE2 plants than in WT under 100 and 150 mM NaCl (**Fig. 7**), indicating the lower ROS accumulation in OE2 plants.

Less root PM depolarization occurred in transgenic Arabidopsis under salt stress

PM depolarization was further determined in the roots of WT and the transgenic plants under salt stress to study the mechanism underlying salt tolerance. As shown in **Fig. 8a**, after 15 min of treatment under 200 mM NaCl, WT root cells showed pronounced DiBAC4(3)-dependent fluorescence signals, while only weak fluorescence could be observed in roots of the three transgenic lines. The relative fluorescence intensity in these lines was about 27–40% of that of WT (**Fig. 8b**), indicating less PM depolarization in the transgenic plants under salt stress. These results further confirmed the roles of SePSS in regulating PM potential under salinity.

Increased K^+ and decreased Na^+ accumulation in transgenic Arabidopsis under salt stress

Considering the role of *SePSS* in regulating PM depolarization under salt stress, which leads to cell K^+ leakage, K^+ and Na^+ contents in roots and leaves from WT and transgenic lines were analyzed. Under control conditions, root K^+ content and root and leaf Na^+ content showed no obvious differences between the transgenic lines and WT, while the leaf K^+ level of transgenic plants was slightly higher than that of WT (**Fig. 9a, b**). As expected, under 150 mM NaCl, more K^+ and less Na^+ were detected in both roots and leaves from transgenic lines than

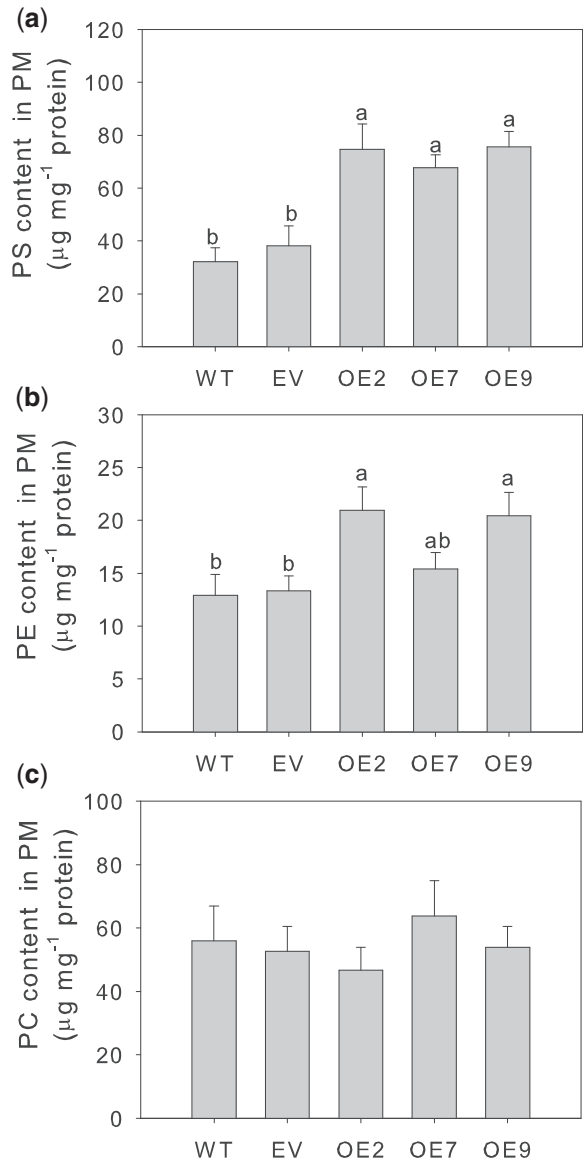

Fig. 5 PS, PE and PC contents in the PM of WT and *SePSS*-overexpressing Arabidopsis plants. PM particles were isolated from leaves of 6-week-old WT and transgenic Arabidopsis plants. Lipids in PM were detected using plant PS/PE/PC ELISA Kits. Values are mean ± SE ($n = 6$). Different letters above the bars indicate significant differences at $P < 0.05$.

those from WT (**Fig. 9a, b**). Thus, the transgenic plants maintained a relatively higher K^+/Na^+ ratio in roots and leaves than WT plants under salt stress (**Fig. 9c**).

Discussion

The mechanism of PS biosynthesis varies between plant species and organs (Marshall and Kates 1974, Delhaize et al. 1999, Yamaoka et al. 2011, Rani et al. 2020). In this study, our results of protein multiple alignments and phylogenetic analysis (**Supplementary Fig. S1**) suggested that the *SePSS* from *S. europaea* encodes a BE-PSS, which catalyzes an exchange reaction between an existing phospholipid head group and Ser (Hübscher et al. 1959). SePSS shares 70% identity with AtPSS1, a BE-PSS from Arabidopsis (Yamaoka et al. 2011), which is the only enzyme responsible for PS biosynthesis found in Arabidopsis till now. In this study, PS levels can be regulated by genetic manipulation of *SePSS*, indicating the important roles of SePSS in PS biosynthesis in *S. europaea*. It is interesting to note that, in the *SePSS*-RNAi callus, the amount of *SePSS* transcript decreased to 3% of that in the EV cells, whereas the PS content in these RNAi calli showed only 15% reduction (**Supplementary Fig. S2**). Therefore, it is very likely that there are other BE-PSS members or the other PS biosynthesis pathway catalyzed by CD-PSS in *S. europaea*, which may contribute to the higher PS content in this species. Both types of PSS activities (BE-PSS and CD-PSS) have also been identified in leek and carrot (Vincent et al. 1999, Manoharan et al. 2000).

PS is synthetized in ER and either transported to the Golgi and then PM via vesicular trafficking (Leventis and Grinstein 2010) or converted to PE by mitochondrial PSD (Shiao et al. 1995, Achleitner et al. 1999). Here, overexpression of *SePSS* in Arabidopsis led to the increase in the PE content (**Fig. 5**), which may be due to the higher PS that can be converted to PE catalyzed by PSD. Previously, overexpression of a wheat *CD-PSS* gene in tobacco and Arabidopsis led to a higher accumulation of PS and directed the cell toward necrotic lesions (Delhaize et al. 1999). Thus, it may be a regulatory mechanism of maintaining the phospholipid homeostasis in the *SePSS*-overexpressing Arabidopsis, as reported previously (Yin et al. 2013).

Although increased PS has been found in several plant species in response to salt stress (Lin and Wu 1996, Wu et al. 2005, Salama and Mansour 2015), what role does PS play and how it works in plant salt tolerance remain unclear. In this study, we found that PS content in PM increased with the increase in NaCl concentration in *S. europaea* (**Fig. 1a**). Particularly, though a greater increase in PS content in Arabidopsis was observed induced by salinity, *S. europaea* showed constitutively much higher PS content and percentage in PM phospholipids than Arabidopsis under either non-salt or salt conditions (**Fig. 1**). It has been documented that specific lipids accumulated constitutively may contribute to the maintenance of membrane structure under salinity in salt-tolerant plant species, and reduced changes in PM lipids induced by salinity are expected to promote the maintenance of membrane integrity and cellular homeostasis in these salt-tolerant species (Mansour 2013). The constitutively higher PS content suggested the role of PS in the salt adaptation of *S. europaea*. Results of salt tolerance analysis in *SePSS*-RNAi *S. europaea* suspension cells and *SePSS*-overexpressing Arabidopsis further confirmed the positive correlation between PS content and plant salt tolerance. Based on our results and the previous studies, several potential roles of PS involved in plant salt tolerance were postulated (**Fig. 10**).

Located in the inner leaflet of the PM, the negatively charged PS contributes to the maintenance of PM polarity with internal electronegative (Delhaize et al. 1999). Therefore, under salt stress, higher PS content may alleviate the PM depolarization to reduce K^+ leakage, which was supported by the less PM depolarization (**Fig. 8**) and higher K^+ content in the *SePSS* transgenic Arabidopsis plants under salt stress (**Figs. 9a, 10**).

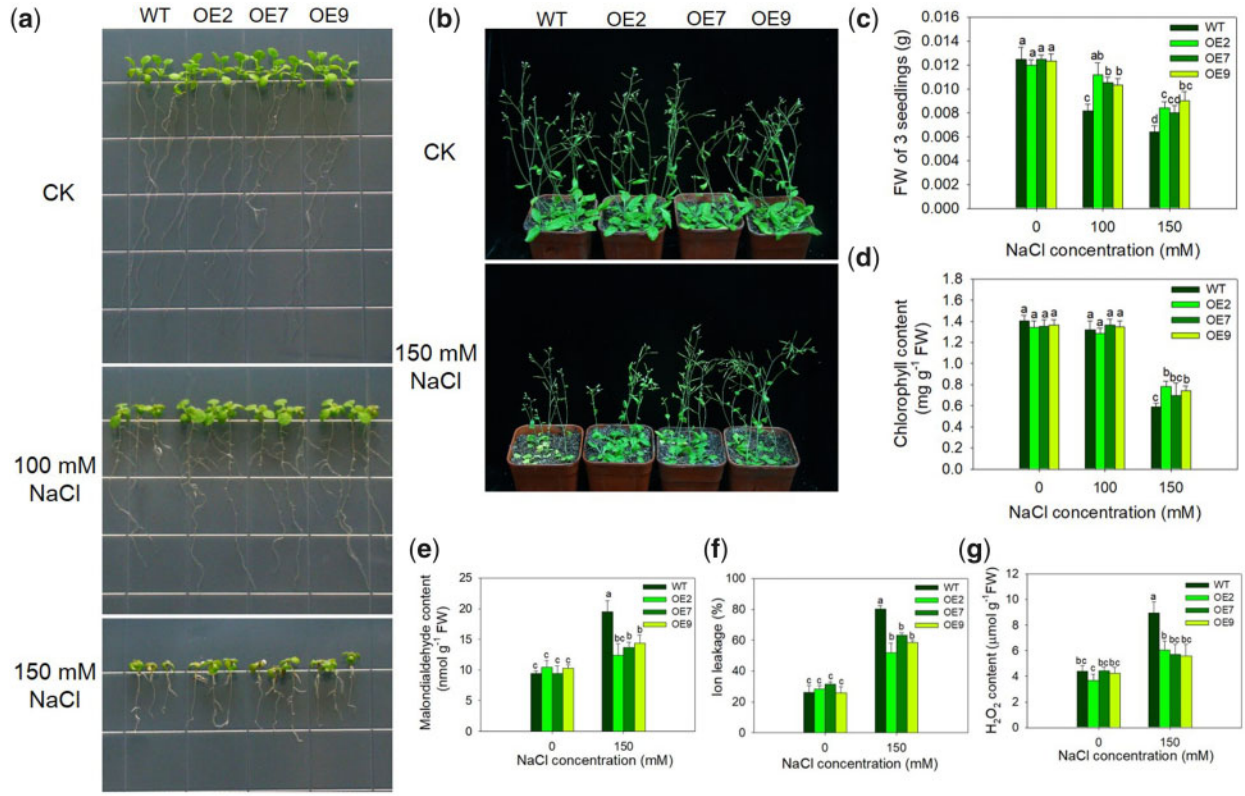

Fig. 6 Overexpression of *SePSS* in Arabidopsis conferred less membrane injury and salt tolerance. Phenotypes and growth parameters of WT and transgenic Arabidopsis seedlings after 8 d of salt treatments: (a) phenotypes, (c) FW and (d) chlorophyll content. Four-day-old seedlings were transferred to the 1/2 MS medium supplied with 0, 100 or 150 mM NaCl for 8 d. Phenotypes (b), MDA levels (e), membrane ion leakage (f) and H_2O_2 content (g) of WT and transgenic Arabidopsis plants. Twenty-one-day-old plants grown in soil were irrigated with 1/2 Hoagland's solution containing 150 mM NaCl. The MDA, ion leakage and H_2O_2 content in leaves were measured after14 d of salt treatment. Values are mean ± SE [$n = 6$ for (c) and (d) and $n = 3$ for (e)–(g)]. Different letters above the bars indicate significant differences at $P < 0.05$.

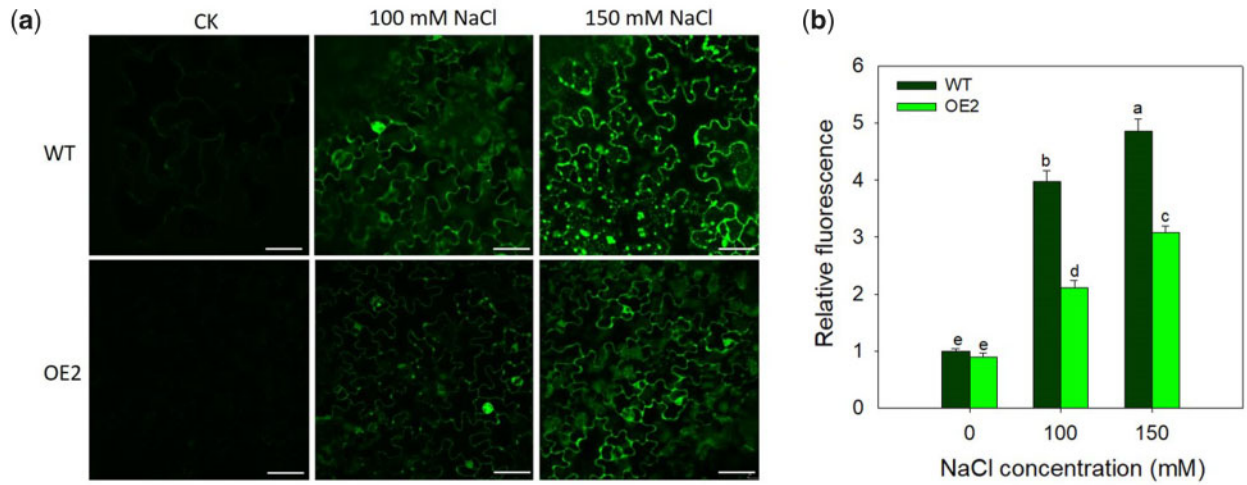

Fig. 7 Relative ROS levels in WT and transgenic Arabidopsis seedlings under salt stress. (a) Confocal images of Arabidopsis leaves stained by H_2DCFDA. Scale bars = 50 μm. (b) Relative H_2DCFDA fluorescence. Four-day-old seedlings from transgenic line OE2 and WT were subjected to 100 and 150 mM NaCl for 48 h. Then, seedlings were vacuum-infiltrated (2 × 5 min) in 10 μM of H_2DCFDA. Leaves were then rapidly rinsed and observed. Values are mean ± SE ($n = 10$). Different letters above the bars indicate significant differences at $P < 0.05$.

On contrary, knockdown of *SePSS* in *S. europaea* cells exacerbated NaCl-induced PM depolarization and led to K^+ efflux (**Fig. 4**). In addition, PS may maintain PM potential through activating PM H^+-ATPase, which contributes to Na^+ efflux by driving PM Na^+/H^+ antiporter and to limiting K^+ efflux by blocking the depolarization-activated outward K^+ channel

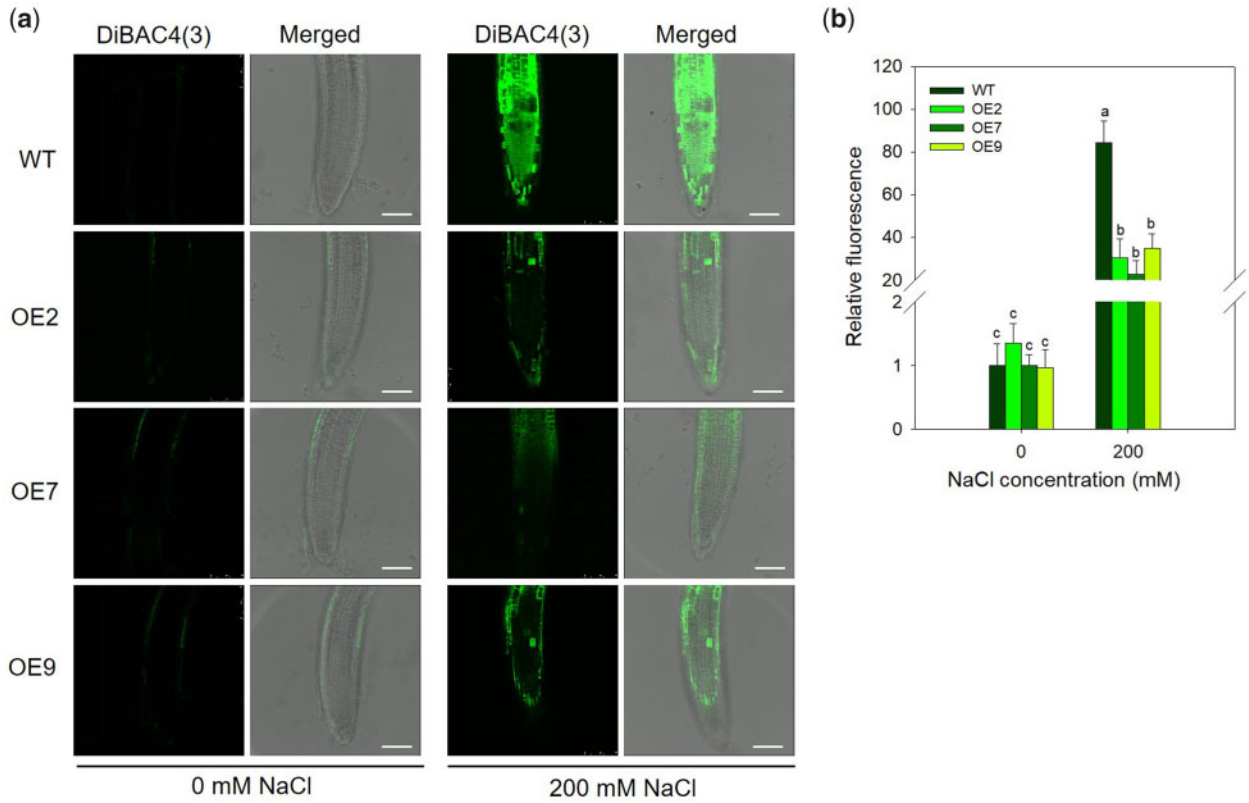

Fig. 8 PM depolarization in WT and transgenic Arabidopsis seedlings under salt stress. Confocal images of root tips stained by DiBAC4(3). Scale bars = 100 μm. (b) Relative DiBAC4(3) fluorescence. Roots of 4-day-old seedlings were incubated in the dark for 15 min with 1 μM DiBAC4(3) in a medium containing 0 and 200 mM NaCl. At least 12 plants were analyzed. Values are mean ± SE (n = 12–15). Different letters above the bars indicate significant differences at $P < 0.05$.

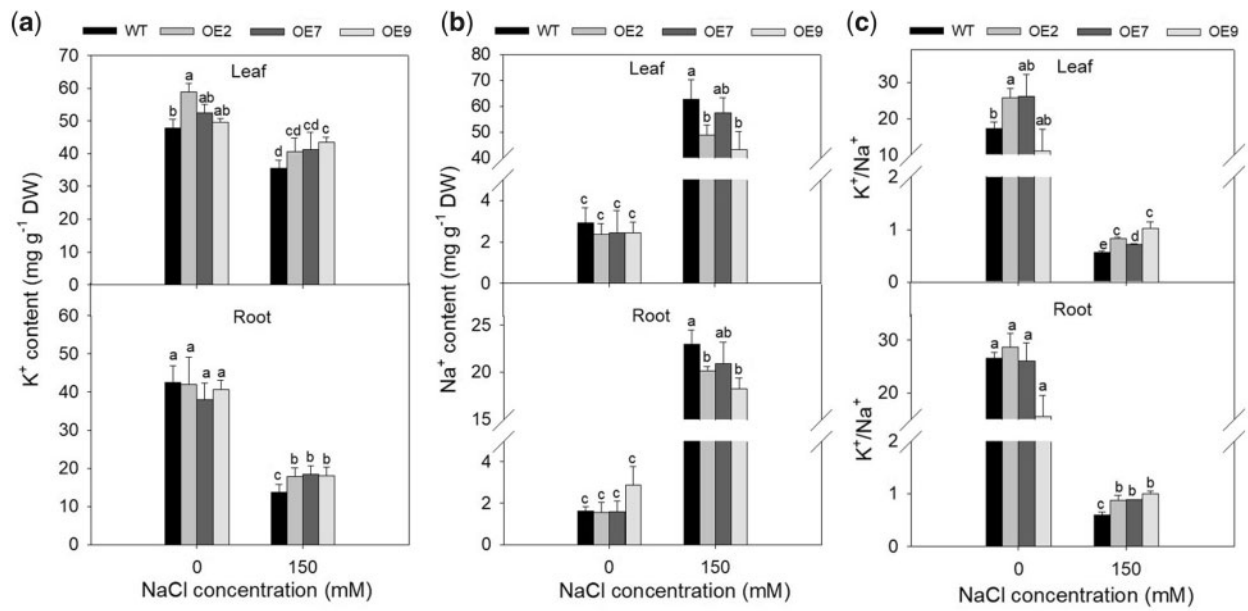

Fig. 9 K^+, Na^+ content and K^+/Na^+ ratio in leaf and root of WT and transgenic Arabidopsis plants. (a) K^+ content, (b) Na^+ content and (c) K^+/Na^+ ratio. Twenty-one-day-old WT and transgenic plants grown in 1/2 Hoagland's solution were transferred to 1/2 Hoagland's solution containing 150 mM NaCl. Ion contents were analyzed in leaves and roots after 7 d of treatment. Values are mean ± SE (n = 3). Different letters above the bars indicate significant differences at $P < 0.05$.

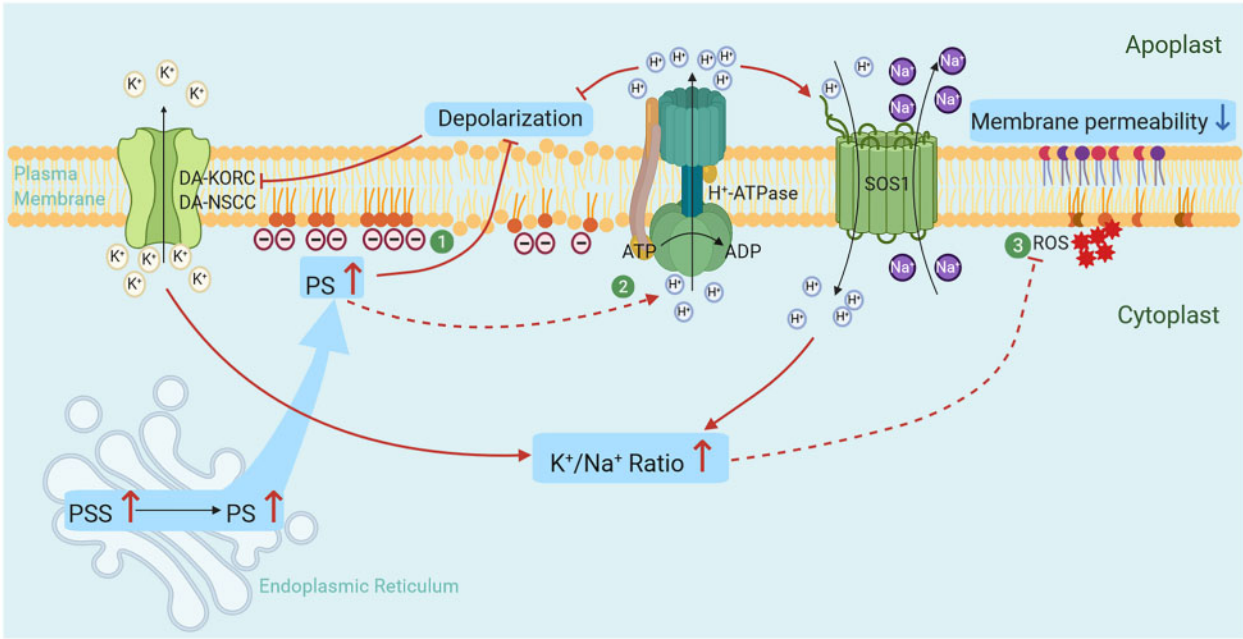

Fig. 10 Schematic representation of PS potential roles in regulating membrane stability and K^+/Na^+ homeostasis in plant cells under salt stress. (1) Increased PS in the inner leaflet of PM due to the upregulation of PSS help maintain a less depolarized membrane potential, which leads to the reduction in DA-KORC- and DA-NSCC-mediated K^+ leakage. (2) Increased PS may promote the activity of PM H^+-ATPase, which sustains an H^+ gradient to drive the SOS1 and also preserves a less depolarized membrane potential, thus promoting Na^+ efflux and restricting K^+ leakage. As a result, the cellular K^+/Na^+ homeostasis is retained. (3) Maintained K^+/Na^+ homeostasis may result in less salt injury and thus less ROS levels, which lead to a less membrane permeability damage.

(**Fig. 10**, Tester and Davenport 2003, Chen et al. 2014). Previous studies discovered that, using the in vitro experimental system, PS promoted PM H^+-ATPase activity in various plant species (Morales-Cedillo et al. 2015, Yu et al. 2019). It has been proposed that the negatively charged polar head groups may accelerate H^+ pumping, which is consistent with the fact that PS is predominantly located on the cytoplasmic side where the catalytic site of the enzyme is found (Harper et al. 1989; Morales-Cedillo et al. 2015). Thus, the higher PS content in *S. europaea* and the transgenic Arabidopsis plants may help maintain K^+/Na^+ homeostasis via maintaining PM potential under salinity (**Fig. 10**).

In addition to PM potential, membrane permeability is impaired by ionic effects and oxidative stress induced by salt stress in salt-sensitive plants (Mansour 2013). ROS induced by salt stress attack membrane lipids and proteins resulting in lipid peroxidation and oxidative damage of proteins, which impairs membrane permeability (Hajlaoui et al. 2009, Tarchoune et al. 2010, Avery 2011). Consistent with these studies, the *SePSS*-overexpressing Arabidopsis plants showed less H_2O_2, ROS and MDA accumulation (**Figs. 6e**, g, 7), coinciding with a lower membrane ion leakage (**Fig. 6f**) than WT, which suggested a less membrane permeability damage in the transgenic plants (**Fig. 10**). The mechanism by which lipid peroxidation increases PM permeability might be that lipid peroxidation products are responsible for ordering phospholipids into the gel phase, which destabilizes the membrane structure (Mansour 2013). Ions leak out from the leaf tissues essentially through membrane transport proteins and also through membrane lipid portion. Therefore, we can infer that the maintained PM potential sustains the activities of membrane transport proteins under salinity to avoid membrane ion leakage in the transgenic plants. On the other hand, the increased PS and PE may also contribute to maintain PM permeability in these transgenic lines. Although no evidence showing the relationship of PS or PE with membrane permeability has been reported, some studies have provided some clues. As one of the bilayer-forming lipids, PS is the only lipid containing very long chains of fatty acids (PS-VLCFAs) in the PM containing >40 carbons (Li et al. 2014), which is believed to maintain the curved shape of the cell membrane (Millar et al. 2000), suggesting its crucial role in maintaining PM structure. In addition, PS molecular species containing VLCFAs were proposed to stabilize ER-derived small vesicles (Sturbois-Balcerzak et al. 1999). Interestingly, PS-VLCFAs were also found to increase significantly under salinity in salt-tolerant sweet potato cultivars (Yu et al. 2019). In addition, the increased amount of PE synthesized by PSD from PS resulted in higher drought tolerance in oat by increasing the flexibility of the membranes (Larsson et al. 2006).

In addition to affecting membrane stability as the membrane component, the role of PS in signaling transduction cannot be ruled out. As a negatively charged phospholipid, PS in PM is involved in recruiting cationic proteins (Yeung et al. 2008). In mammals, a number of proteins have been found interact with PS (Vance and Steenbergen 2005), including annexin V (Swairjo et al. 1995), protein kinase C (Sutton and Sprang 1998), phospholipase C (Singh et al. 2015), and synaptotagmin (Zhang et al. 2009), whose homologs are reportedly

involved in plant salt tolerance (Schapire et al. 2008, Laohavisit et al. 2013, Meringer et al. 2016). Most recently, Platre et al. (2019) reported that Rho of Plants 6 was stabilized by PS into PM nanodomains, which are required for auxin signaling, and variations in PS levels were supposed to act as a physiological regulator of small GTPase signaling during plant development. Further investigations on the interaction of PS and proteins involved in plant salt tolerance will benefit our understanding of PS roles in signaling transduction.

As the biological barrier of cells, PM protects the contents of cells from biotic and abiotic stress. In addition to salinity, a wide range of environmental stresses, including extreme temperature, drought, heavy metals, herbivory and pathogens, can also lead to PM impairment (Chen et al. 2020). Therefore, maintaining PM stability and integrity may be a global defense mechanism that evolved in plants exposed to these environmental stresses. Inconsistent with this hypothesis, the *SePSS*-overexpressing Arabidopsis seedlings showed better growth under either drought stress mimicked by 250 mM sorbitol treatment or 20 μM of cadmium (Cd) stress (**Supplementary Fig. S4**). Thus, our work may provide a potential strategy for improving plant growth under multiple stresses, which has drawn wide attention in recent years.

In summary, our results suggested that constitutively high PS content contributes to the salt tolerance of *S. europaea*. SePSS was involved in plant salt tolerance by regulating PS levels. Increased PS content resulted in the maintenance of PM depolarization and membrane permeability, hence PM stability, which help maintain K^+/Na^+ homeostasis under salinity. Considering the properties of PM, our work may provide a potential strategy for improving plant growth under multiple stresses. Further investigations on proteins that can interact with PS will promote our understanding of PS roles in plant salt tolerance. In addition, future researches on the membrane lipid remodeling patterns of *S. europaea* in response to salinity could provide important insight into the roles of other lipids and the salt adaptation mechanism of this species.

Materials and Methods

Plant material and growth conditions

Salicornia europaea seeds were collected from coastal areas of Dongying City, Shandong Province of China. The plants were grown in a greenhouse at 25/20°C (day/night) with a relative humidity of 50–60% and a photoperiod of 16/8 h (light/dark). After germination, seedlings were irrigated weekly with 1/2 Hoagland's solution (Hoagland and Arnon 1950) for 21 d. For PM PS content analysis, seedlings were then irrigated by 1/2 Hoagland's solution containing 200, 400, 600 and 800 mM NaCl for 2 weeks. Plants irrigated with 1/2 Hoagland's solution served as the control.

Arabidopsis *thaliana* (ecotype Columbia-0) plants were grown in plastic pots containing a mixture of vermiculite, turf and humus (1:1:1, by vol), in a growth chamber at 23 ± 1°C under a photoperiod of 16/8 h (light/dark). For PM PS content analysis, 21-day-old seedlings were treated with 100 and 200 mM NaCl solution for 2 weeks. Plants irrigated with 1/2 Hoagland's solution served as the control.

PM isolation and lipid analysis

PM was isolated as previously reported (Tang 2012). About 30 g of *S. europaea* shoots, calli or Arabidopsis leaves were homogenized in grinding buffer (pH 7.5) (25 mM 2-[4-(2-hydroxyethyl) piperazin-1-yl] ethanesulfonic acid (HEPES), 0.33 M sucrose, 10% glycerol, 0.6% PVP, 5 mM ascorbic acid, 5 mM ethylene diamine tetraacetic acid (EDTA), 5 mM dithiothreitol (DTT) and 1 mM phenylmethanesulfonyl fluoride (PMSF)). After filtered through Miracloth and centrifuged at 10,000 × *g* for 15 min, the supernatant was centrifuged at 80 000 × *g* for 1 h and the total microsomal fractions were resuspended. Two-phase partitioning was performed using two kinds of solutions containing 8.27% or 6.2% polyethylene glycol (PEG) 3350 and dextran T-500 with 0.33 M sucrose, 3 mM KCl and 5 mM KH_2PO_4/K_2HPO_4 buffer (pH 7.8). After partitioning, the upper phase fraction was diluted with 10 volumes of dilution buffer (0.33 M sucrose, 25 mM HEPES and 1 mM DTT) and spun at 120 000 × *g* for 1 h to collect the PMs. The pellets were resuspended in 100 μl of suspension buffer (5 mM KH_2PO_4/K_2HPO_4, pH 7.8, 3 mM KCl, 1 mM DTT, 0.1 mM EDTA and 1 μM protease cocktail). The protein concentration was determined using the Bradford method.

Lipid extraction was performed as described by Welti et al. (2002). PM particles in the aqueous solution were extracted with chloroform/methanol (v/v, 2:1) containing 0.01% butylated hydroxytoluene three times with 30 min of agitation each time. Wash the combined lower layers once with 1 ml of 1 M KCl and once with 1 ml of water.

For the PM PS determination, PM lipid samples from *S. europaea* shoots and Arabidopsis leaves were analyzed on a triple quadrupole MS/MS equipped for ESI according to Welti et al. (2002) by Kansas Lipidomics Research Center (**http://www.k-state.edu/lipid/lipidomics**).

For the PM lipid analysis in *S. europaea* suspension cells and transgenic Arabidopsis plants, plant PS/PE/PC ELISA Kits (R&D Systems, Minnesota, USA) were used according to the manufacturer's instructions. The intensity of the reaction solution color was measured at 450 nm using a spectrophotometer. The calibration standards were assayed at the same time as the samples were assayed and allow the operator to produce a standard curve of optical density (OD) vs. PS/PE/PC concentration. The concentration of PS/PE/PC in the samples was then determined by comparing the OD of the samples to the standard curve. Six replicates were performed.

Gene isolation and sequence analysis of SePSS

Total RNA was extracted from 1-month-old *S. europaea* shoot with TRIzol reagent (Transgen, Beijing, China). After RNase-free DNase I (Fermentas, Vilnius, Lithuania) digestion, the first-strand cDNA was synthesized by TransScript II reverse transcriptase (Transgen) following the manufacturers' instructions. The full length of *SePSS* cDNA was amplified, subcloned into pEASY-T1 Simple vector (Transgen) and sequenced. Primers used for gene amplification are shown in **Supplementary Table S1**.

Multiple protein alignments and the unrooted neighbor-joining phylogenetic tree were performed using Clustal Omega (**https://www.ebi.ac.uk/Tools/msa/clustalo/**). The protein transmembrane domains were analyzed by TMHMM Server 2.0. (https://services.healthtech.dtu.dk/service.php?TMHMM-2.0).

Microscopy observation of SePSS subcellular localization

The coding sequence of *SePSS* was subcloned into the *Bam*HI sites of pCAMBIA1300-35S::GFP vector to form GFP fusion constructs. The encoding sequence of ER marker HDEL (CATGATGAGCTT) was fused 'in-frame' with the mCherry reporter gene under the control of the cauliflower mosaic virus (CaMV) 35S promoter to form pCAMBIA2300-HDEL-mCherry. Primers used for vector construction are shown in **Supplementary Table S1**. For transient expression in tobacco, the recombinant plasmids were transformed into *Agrobacterium tumefaciens* strain C58 and then infiltrated into tobacco leaves. After infiltration, plants were placed in the growth chamber for 2 d, followed by live-cell imaging under a confocal laser scanning microscope (LSM-510, Zeiss, Germany). The 488- and 587-nm lasers were used for GFP and mCherry, respectively.

Expression analysis of *SePSS* by qRT-PCR

One-month-old plants were treated with 1/2 Hoagland's solution containing 200 or 800 mM NaCl. Plants grown in 1/2 Hoagland's solution served as the controls. Shoots from at least three plants under each treatment were sampled

at 0, 6, 12, 24 and 72 h. The total RNA and cDNA were prepared from the samples using the method mentioned above. SYBR Green Realtime PCR Master Mix (Toyobo, Osaka, Japan) was used to detect gene expression by an Mx3000P™ Real-Time PCR System (Agilent, CA, USA). The relative gene expression levels were calculated by the $2^{-\Delta\Delta Ct}$ method (Livak and Schmittgen 2001) with the α-*Tubulin* gene from *S. europaea* as an internal control. Each sample was repeated thrice, and three biological experiments were performed. Primers are shown in **Supplementary Table S1**.

Salicornia europaea callus transformation and suspension cell culture

Plasmid pU1301 containing a hairpin motif of the *SePSS* gene was used for RNAi. Primers used for vectors construction are shown in **Supplementary Table S1**. *Agrobacterium*-mediated transformation of *S. europaea* callus and suspension cell culture was performed according to our previous report (Tai et al. 2017).

Friable calli were infected by *A. tumefaciens* C58 containing the construct of pU1301-*SePSS*-RNAi to obtain a *SePSS* knockdown callus. Plasmid pU1301 was also transformed to *S. europaea* callus to act as an EV control. After 3 d of cocultivation on solid callus induction medium (CIM) in the dark at 22°C, callus cultures were washed with liquid CIM supplemented with 100 mg l^{-1} timentin (TMT) and then cultured in solid CIM with 100 mg l^{-1} TMT for another 3 d to suppress the bacteria. Then, the calli were transferred to the selective mediums (CIM containing 100 mg l^{-1} TMT and 25 mg l^{-1} hygromycin) for 3 weeks. Surviving calli were further subcultured onto the same medium for 3–4 cycles of selection.

Cell suspension cultures were established from friable calli. About 1.0 g of calli were transferred to 250-ml conical flask containing 100 ml of liquid callus selection medium. Flasks were incubated on a reciprocating shaker (120 rpm) at 26°C in the dark for 15–20 d. The cultures were supplied with fresh medium after every 10–15 d.

Gene expression analysis in transgenic *S. europaea* suspension cells and Arabidopsis lines

After 3–4 cycles of selection by hygromycin, the surviving calli transformed with pU1301-*SePSS*-RNAi and pU1301 were used to detect the expression of *SePSS* by qRT-PCR. The gene α-*Tubulin* from *S. europaea* served as an internal control.

For *SePSS* and *AtPSDs* expression analyses, leaves of 21-day-old WT and transgenic Arabidopsis lines were sampled. The *AtActin* gene was used as an internal control. Vertical bars indicate ± SE of three replicates on one sample. Each sample was repeated thrice, and three biological experiments were performed. Primers are shown in **Supplementary Table S1**.

Salt tolerance analysis in suspension cells

The impact of NaCl on cell viability was determined by the method of FDA–PI simultaneous staining according to Jones and Senft (1985). FDA, a nonpolar ester, passes through cell membranes and is hydrolyzed by intracellular esterases to produce fluorescein, which passes slowly through a living cell membrane, accumulates inside the cell and exhibits green fluorescence when excited by blue light. Thus, cells fluorescing bright green are considered viable. PI, an analog of ethidium bromide, passes through only damaged cell membranes and intercalates with DNA and RNA to form a bright red fluorescent complex. Therefore, cells fluorescing bright red are nonviable cells. Cell viability is represented by the percentage of viable cells fluorescing green. After treated with NaCl (0, 400 and 800 mM) for 8 h, the samples were stained with 5 μM FDA and 10 μM PI in the dark for 40 min. The excitation and emission wavelengths for the FDA were 488 and 500–530 nm, while those of PI were 543 and 600–750 nm. The evaluation of viability was conducted by a confocal microscopy (LSM-510). Cells from at least 10 microscope fields under 20× objective were analyzed.

Measurement of PM depolarization

PM depolarization was monitored using the voltage-sensitive fluorescent probe DiBAC4(3) (Sigma-Aldrich; Konrad and Hedrich 2008), which permeates the cell membrane and accumulates in the cytosol upon membrane depolarization. DiBAC4(3) has a fluorescence intensity in the aqueous solution that increases several folds in a milieu like a cytoplasm (Bräuner et al. 1984). *Salicornia europaea* suspension cells of *SePSS*-RNAi and the EV controls were incubated in the dark for 15 min with 1 μM DiBAC4(3) in a medium containing 0, 400 and 800 mM NaCl. Cells were maintained under shaking during the incubation. Fluorescence was detected and imaged under a confocal microscope (LSM-510). The fluorophore was excited at 488 nm, and the emission was detected between 500 and 550 nm. The average fluorescence intensity of cells was calculated by ImageJ 1.49 (Image Processing and Analysis in Java, **http://imagej.net**). Cells from at least 10 microscope fields under 20× objective were analyzed.

For assays in Arabidopsis, sterilized seeds of WT and transgenic lines were sown on a medium containing 1/2 MS salts, with 1% (w/v) sucrose and 1% (w/v) agar, stratified at 4°C in the dark for 2 d. Roots of 4-day-old seedlings were incubated in the dark for 15 min with 1 μM DiBAC4(3) in a medium containing 0 and 200 mM NaCl. At least 12 plants were analyzed.

K^+ fluxes measurement

Net K^+ fluxes were measured in the Younger USA (Beijing) BioFunction Institute using Non-invasive Micro-test Technology (NMT100 Series; YoungerUSA LLC, Amherst, MA, USA). After treated by 0, 400 and 800 mM NaCl for 2 h, *S. europaea* cells were placed at the center of the coverslip treated with 0.008% (w/v) poly-L-Lys. After adhering to the coverslip (approximately 15 min), cells were stabilized in the measuring solution (0.5 mM KCl, 0.1 mM NaCl, 0.2 mM $CaCl_2$, 0.1 mM $MgCl_2$, 2.5% sucrose with pH 5.7) for 10 min before measurement. For K^+ flux measurement, 3 ml of measuring solution was added slowly to the container. K^+ fluxes of the sample cells were recorded for 5 min. Net K^+ fluxes were calculated using JCal V3.3 (a free MS Excel spreadsheet; **http://youngerusa.com** or **http://xuyue.net**).

Arabidopsis transformation and salt tolerance analysis

The complete open reading frames of *SePSS* was subcloned into the *Bam*HI sites of the expression vector pSN1301 downstream of the CaMV 35S promoter. The constructs were then introduced into *A. tumefaciens* C58. The transformation of Arabidopsis was carried out by the floral-dip method. The T1 transgenic plants were selected on 1/2 MS agar plates containing 25 mg l^{-1} hygromycin. Seeds from each T1 plant were individually collected. Selected T2 plants were propagated, and homozygous overexpression lines were confirmed by qRT-PCR. In this study, three *SePSS*-overexpression lines (OE2, 7 and 9) were used for further experiments.

For salt treatments, sterilized seeds of WT and transgenic lines were sown on a medium containing 1/2 MS salts, with 1% (w/v) sucrose and 1% (w/v) agar, stratified at 4°C in the dark for 2 d. Four-day-old seedlings were transferred to the 1/2 MS medium supplied with 100 or 150 mM NaCl. Seedlings grown in 1/2 MS medium served as the control. Measurements for chlorophyll content and plant FW were taken at 8 d after treatment. In addition, 21-day-old plants grown in soil were irrigated with 1/2 Hoagland's solution containing 150 mM NaCl. MDA content, membrane ion leakage and H_2O_2 content in leaves were measured after 14 d of salt treatment.

Leaf chlorophyll was extracted with 80% acetone (v/v), and the total chlorophyll content was determined spectrophotometrically according to Arnon (1949). The MDA content was determined according to Peever and Higgins (1989). The ion leakage from the cellular membranes was determined via conductivity measurements. Ion leakage expressed as a percentage was calculated as described previously (Fan et al. 1997). The H_2O_2 content in leaves was determined based upon the peroxide-mediated oxidation of Fe^{2+}, followed by the reaction of Fe^{3+} with xylenol orange [*o*-cresolsulfonephthalein 3′,3″bis(methylimino)diacetic acid, sodium salt] as described by Bellincampi et al. (2000).

ROS measurement

ROS accumulation was detected using the fluorescent probe H_2DCFDA (Sigma-Aldrich) as described by L'Haridon et al. (2011). Four-day-old seedlings from transgenic line OE2 and WT were subjected to 100 and 150 mM NaCl for 48 h. Then, seedlings were vacuum-infiltrated (2 × 5 min) in 10 μM of H_2DCFDA. Leaves were then rapidly rinsed and observed under a confocal microscopy (LSM-510) with excitation at 488 nm. The fluorescence intensity was quantified with ImageJ 1.49. At least 10 microscope fields under 20× objective were analyzed.

Na^+ and K^+ measurements

For ion measurements, 21-day-old WT and transgenic plants grown in 1/2 Hoagland's solution were transferred to 1/2 Hoagland's solution containing 150 mM NaCl. After 7 d of treatment, roots and rosettes were harvested separately, dried at 70°C for 48 h and ground into fine powder in an MM400 mixer mill (Retsch GmbH, Germany). About 10–20 mg of tissue powder was digested with the mixture of nitric acid and hydrogen peroxide using an optimized microwave vacuum tissue processing system (MARS, CEM, NC, USA). The digested samples were used to determine Na^+ and K^+ contents by an atomic emission spectroscopy (ICP-AES; Thermo Scientific, New York, USA).

Statistical analysis

All statistical analyses were performed with SPSS18.0. Data were analyzed by one-way ANOVA and presented in the form of mean ± standard error (SE).

Supplementary Data

Supplementary data are available at PCP online.

Acknowledgments

This work was supported by the Research Programs from the Chinese Ministry of Agriculture (No. 2016ZX08009-003-002) and the Major Science and Technology Innovation Project of Shandong Province (No. 2019JZZY010726). We thank Jingquan Li from the Plant Science Facility of the Institute of Botany, Chinese Academy of Sciences, for her excellent technical assistance with the confocal microscopy observation.

Disclosures

The authors have no conflicts of interest to declare.

References

Achleitner, G., Gaigg, B., Krasser, A., Kainersdorfer, E., Kohlwein, S.D., Perktold, A., et al. (1999) Association between the endoplasmic reticulum and mitochondria of yeast facilitates interorganelle transport of phospholipids through membrane contact. *Eur. J. Biochem.* 264: 545–553.

Alvarez-Pizarro, J.C., Gomes-Filho, E., de Lacerda, C.F., Alencar, N.L.M. and Prisco, J.T. (2009) Salt-induced changes on H^+-ATPase activity, sterol and phospholipid content and lipid peroxidation of root plasma membrane from dwarf-cashew (*Anacardium occidentale* L.) seedlings. *Plant Growth Regul.* 59: 125–135.

Apel, K. and Hirt, H. (2004) Reactive oxygen species: metabolism, oxidative stress, and signal transduction. *Annu. Rev. Plant Biol.* 55: 373–399.

Arnon, D.I. (1949) Copper enzymes in isolated chloroplasts. Polyphenoloxidase in *Beta vulgaris*. *Plant Physiol.* 24: 1–15.

Avery, S.V. (2011) Molecular targets of oxidative stress. *Biochem. J.* 434: 201–210.

Bräuner, T., Hülser, D.F. and Strasser, R.J. (1984) Comparative measurements of membrane potentials with microelectrodes and voltage-sensitive dyes. *Biochim. Biophys. Acta* 771: 208–216.

Bellincampi, D., Dipierro, N., Salvi, G., Cervone, F. and De Lorenzo, G. (2000) Extracellular H_2O_2 induced by oligogalacturonides is not involved in the inhibition of the auxin-regulated *rolB* gene expression in tobacco leaf explants. *Plant Physiol.* 122: 1379–1385.

Cheeseman, J.M. (2007) Hydrogen peroxide and plant stress: a challenging relationship. *Plant Stress* 1: 4–15.

Chen, S., Hawighorst, P., Sun, J. and Polle, A. (2014) Salt tolerance in Populus: significance of stress signaling networks, mycorrhization, and soil amendments for cellular and whole-plant nutrition. *Environ. Exp. Bot.* 107: 113–124.

Chen, Y., Cao, C., Guo, Z., Zhang, Q., Li, S., Zhang, X., et al. (2020) Herbivore exposure alters ion fluxes and improves salt tolerance in a desert shrub. *Plant Cell Environ.* 43: 400–419.

Chen, Z., Newman, I., Zhou, M., Mendham, N., Zhang, G. and Shabala, S. (2005) Screening plants for salt tolerance by measuring K^+ flux: a case study for barley. *Plant Cell Environ.* 28: 1230–1246.

Delhaize, E., Hebb, D.M., Richards, K.D., Lin, J.M., Ryan, P.R. and Gardner, R.C. (1999) Cloning and expression of a wheat (*Triticum aestivum* L.) phosphatidylserine synthase cDNA. *J. Biol. Chem.* 274: 7082–7088.

Dionisio-Sese, M.L. and Tobita, S. (1998) Antioxidant responses of rice seedlings to salinity stress. *Plant Sci.* 135: 1–9.

Fan, L., Zheng, S. and Wang, X. (1997) Antisense suppression of phospholipase Da retards abscisic acid- and ethylene promoted senescence of postharvest *Arabidopsis* leaves. *Plant Cell* 9: 2183–2196.

Fan, P.X., Nie, L.L., Jiang, P., Feng, J.J., Lv, S.L., Chen, X.Y., et al. (2013) Transcriptome analysis of *Salicornia europaea* under saline conditions revealed the adaptive primary metabolic pathways as early events to facilitate salt adaptation. *PLoS One* 8: e80595.

Flowers, T.J. and Colmer, T.D. (2008) Salinity tolerance in halophytes. *New Phytol.* 179: 945–963.

Guo, Q., Liu, L. and Barkla, B.J. (2019) Membrane lipid remodeling in response to salinity. *Int. J. Mol. Sci.* 20:4264.

Hajlaoui, H., Denden, M. and Elyeb, N. (2009) Changes in fatty acids composition, hydrogen peroxide generation and lipid peroxidation of salt-stressed corn (*Zea mays* L.) root. *Acta Physiol. Plant.* 31: 33–34.

Harper, J.F., Surowy, T.K. and Sussman, M.R. (1989) Molecular cloning and sequence of cDNA encoding the plasma membrane proton pump (H^+-ATPase) of *Arabidopsis thaliana*. *Proc. Natl. Acad. Sci. USA* 86: 1234–1238.

Hoagland, D.R. and Arnon, D.I. (1950) The water-culture method for growing plants without soil. *Calif. Agric. Exp. Stn.* 347: 1–32.

Hübscher, H.G., Dils, R.R. and Pover, W.F.R. (1959) Studies on the biosynthesis of phosphatidylserine. *Biochim. Biophys. Acta* 36: 518–525.

Jones, K.H. and Senft, J.A. (1985) An improved method to determine cell viability by simultaneous staining with fluorescein diacetate-propidium iodide. *J. Histochem. Cytochem.* 33: 77–79.

Konrad, K.R. and Hedrich, R. (2008) The use of voltage-sensitive dyes to monitor signal-induced changes in membrane potential-ABA triggered membrane depolarization in guard cells. *Plant J.* 55: 161–173.

L'Haridon, F., Besson-Bard, A., Binda, M., Serrano, M., Abou-Mansour, E., Balet, F., et al. (2011) A permeable cuticle is associated with the release of reactive oxygen species and induction of innate immunity. *PLoS Pathog.* 7: e1002148.

Laohavisit, A., Richards, S.L., Shabala, L., Chen, C., Colaço, R.D., Swarbreck, S. M., et al. (2013) Salinity-induced calcium signaling and root adaptation in Arabidopsis require the calcium regulatory protein annexin1. *Plant Physiol.* 163: 253–262.

Larsson, K.E., Nystrom, B. and Liljenberg, C. (2006) A phosphatidylserine decarboxylase activity in root cells of oat (*Avena sativa*) is involved in altering membrane phospholipid composition during drought stress acclimation. *Plant Physiol. Biochem.* 44: 211–219.

Leventis, P.A. and Grinstein, S. (2010) The distribution and function of phosphatidylserine in cellular membranes. *Annu. Rev. Biophys.* 39: 407–427.

Li, Y., Zheng, G., Jia, Y., Yu, X., Zhang, X., Yu, B., et al. (2014) Acyl chain length of phosphatidylserine is correlated with plant lifespan. *PLoS One* 9: e103227.

Lin, H. and Wu, L. (1996) Effects of salt stress on root plasma membrane characteristics of salt-tolerant and salt-sensitive buffalograss clones. *Environ. Exp. Bot.* 36: 239–254.

Liu, C., Yin, H., Gao, P., Hu, X., Yang, J., Liu, Z., et al. (2013) *PHOSPHATIDYLSERINE SYNTHASE1* is required for inflorescence meristem and organ development in *Arabidopsis*. *J. Integr. Plant Biol.* 55: 682–695.

Livak, K.J. and Schmittgen, T.D. (2001) Analysis of relative gene expression data using real-time quantitative PCR and the 2(−Delta Delta C(T)) method. *Methods* 25: 402–408.

Lv, S.L., Jiang, P., Chen, X.Y., Fan, P.X., Wang, X.C., Fan, P., et al. (2012) Multiple compartmentalization of sodium conferred salt tolerance in *Salicornia europaea*. *Plant Physiol. Biochem.* 51: 47–e52.

Ma, J., Cheng, Z., Chen, J., Shen, J., Zhang, B., Ren, Y., et al. (2016) Phosphatidylserine synthase controls cell elongation especially in the uppermost internode in rice by regulation of exocytosis. *PLoS One* 11: e0153119.

Manoharan, K., Chae, H.S., Myoung, J., Cho, S.H., Shin, S.H., Cho, B.H., et al. (2000) Synthesis of phosphatidylserine in carrot cells cultured under carbon-source starvation. *Plant Cell Physiol.* 41: 1143–1148.

Mansour, M.M.F. (2013) Plasma membrane permeability as an indicator of salt tolerance in plants. *Biol. Plant.* 57: 1–10.

Marshall, M.O. and Kates, M. (1974) Biosynthesis of nitrogenous phospholipids in spinach leaves. *Can. J. Biochem.* 52: 469–482.

Matsumoto, K. (1997) Phosphatidylserine synthase from bacteria. *Biochim. Biophys. Acta* 1348: 214–227.

Meringer, M., Villasuso, A.L., Margutti, M.P., Usorach, J., Pasquare, S.J., Giusto, N., et al. (2016) Saline and osmotic stresses stimulate PLD/diacylglycerol kinase activities and increase the level of phosphatidic acid and proline in barley roots. *Environ. Exp. Bot.* 128: 69–78.

Millar, A.A., Smith, M.A. and Kunst, L. (2000) All fatty acids are not equal: discrimination in plant membrane lipids. *Trends Plant Sci.* 5: 95–101.

Morales-Cedillo, F., Gonzalez-Solis, A., Gutierrez-Angoa, L., Cano-Ramőrez, D.L. and Gavilanes-Ruiz, M. (2015) Plant lipid environment and membrane enzymes: the case of the plasma membrane H^+-ATPase. *Plant Cell Rep.* 34: 617–629.

Nakamura, Y. (2017) Plant phospholipid diversity: emerging functions in metabolism and protein–lipid interactions. *Trends Plant Sci.* 22: 1027–1037.

Nerlich, A., von Orlow, M., Rontein, D., Hanson, A.D. and Dormann, P. (2007) Deficiency in phosphatidylserine decarboxylase activity in the *psd1 psd2 psd3* triple mutant of Arabidopsis affects phosphatidylethanolamine accumulation in mitochondria. *Plant Physiol.* 144: 904–914.

Nocito, F.F., Sacchi, G.A. and Cocucci, M. (2002) Membrane depolarization induces K^+ efflux from subapical maize root segments. *New Phytol.* 154: 45–51.

Ohsawa, T., Nishijima, M. and Kuge, O. (2004) Functional analysis of Chinese hamster phosphatidylserine synthase 1 through systematic alanine mutagenesis. *Biochem. J.* 381: 853–859.

Peever, T.L. and Higgins, V.J. (1989) Electrolyte leakage, lipoxygenase, and lipid peroxidation induced in tomato leaf tissue by specific and non specific elicitors from *Cladosporium fluvum*. *Plant Physiol.* 90: 867–875.

Platre, M.P., Bayle, V., Armengot, L., Bareille, J., Marquès-Bueno, M.M., Creff, A., et al. (2019) Developmental control of plant Rho GTPase nano-organization by the lipid phosphatidylserine. *Science* 364: 57–62.

Rani, M.H., Liu, Q., Yu, N., Zhang, Y., Wang, B., Cao, Y., et al. (2020) *ES5* is involved in the regulation of phosphatidylserine synthesis and impacts on early senescence in rice. *Plant Mol. Biol.* 102: 501–515.

Roelfsema, M.R.G., Steinmeyer, R., Staal, M. and Hedrich, R. (2001) Single guard cell recordings in intact plants: light-induced hyperpolarization of the plasma membrane. *Plant J.* 26: 1–13.

Salama, K.H.A. and Mansour, M.M.F. (2015) Choline priming-induced plasma membrane lipid alterations contributed to improved wheat salt tolerance. *Acta Physiol. Plant.* 37: 1–7.

Salama, K.H.A., Mansour, M.M.F., Ali, F.Z.M. and Abou-Hadid, A.F. (2007) NaCl-induced changes in plasma membrane lipids and proteins of *Zea mays* L. cultivars differing in their response to salinity. *Acta Physiol. Plant.* 29: 351–359.

Schapire, A.L., Voigt, B., Jasik, J., Rosado, A., Lopez-Cobollo, R., Menzel, D., et al. (2008) *Arabidopsis Synaptotagmin 1* is required for the maintenance of plasma membrane integrity and cell viability. *Plant Cell* 20: 3374–3388.

Shabala, L., Cuin, T.A., Newman, A. and Shabala, S. (2005) Salinity-induced ion flux patterns from the excised roots of *Arabidopsis sos* mutants. *Planta* 222: 1041–1050.

Shiao, Y.J., Lupo, G. and Vance, J.E. (1995) Evidence that phosphatidylserine is imported into mitochondria via a mitochondria-associated membrane and that the majority of mitochondrial phosphatidylethanolamine is derived from decarboxylation of phosphatidylserine. *J. Biol. Chem.* 270: 11190–11198.

Singh, A., Bhatnagar, N., Pandey, A. and Pandey, G.K. (2015) Plant phospholipase C family: regulation and functional role in lipid signaling. *Cell Calcium* 58: 139–146.

Sturbois-Balcerzak, B., Vincent, P., Maneta-Peyret, L., Duvert, M., SatiatJeunemaitre, B., Cassagne, C., et al. (1999) ATP-dependent formation of phosphatidylserine-rich vesicles from the endoplasmic reticulum of leek cells. *Plant Physiol.* 120: 245–256.

Sutton, R.B. and Sprang, S.R. (1998) Structure of the protein kinase Cb phospholipid-binding C2 domain complexed with Ca^{2+}. *Structure* 6: 1395–1405.

Swairjo, M.A., Concha, N.O., Kaetzel, M.A., Dedman, J.R. and Seaton, B.A. (1995) Ca^{2+}-bridging mechanism and phospholipid head group recognition in the membrane-binding protein annexin V. *Nat. Struct. Mol. Biol.* 2: 968–974.

Tai, F., Lv, S.L., Jiang, P., Wang, J.H., Feng, J.J. and Li, Y.X. (2017) Establishment of a gene function analysis system for the euhalophyte *Salicornia europaea* L. *Plant Cell Rep.* 36: 1251–1261.

Tang, W. (2012) Quantitative analysis of plasma membrane proteome using two-dimensional difference gel electrophoresis. *Methods Mol. Biol.* 876: 67–82.

Tarchoune, I., Sgherri, C., Izzo, R., Lachaal, M., Ouerghi, Z. and Navari-Izzo, F. (2010) Antioxidative response of *Ocimum basilicum* to sodium chloride and sodium sulphate salinization. *Plant Physiol. Biochem.* 48: 772–777.

Tester, M. and Davenport, R. (2003) Na^+ tolerance and Na^+ transport in higher plants. *Ann. Bot.* 91: 503–527.

Vance, J.E. (2008) The matic review series: glycerolipids. Phosphatidylserine and phosphatidylethanolamine in mammalian cells: two metabolically related aminophospholipids. *J. Lipid Res.* 49: 1377–1387.

Vance, J.E. and Steenbergen, R. (2005) Metabolism and functions of phosphatidylserine. *Prog. Lipid Res.* 44: 207–234.

Vincent, P., Maneta-Peyret, L., Sturbois-Balcerzak, B., Duvert, M., Cassagne, C. and Moreau, P. (1999) One of the origins of plasma membrane phosphatidylserine in plant cells is a local synthesis by a serine exchange activity. *FEBS Lett.* 464: 80–84.

Wang, X.C., Fan, P.X., Song, H.M., Chen, X.Y., Li, X.F. and Li, Y.X. (2009) Comparative proteomic analysis of differentially expressed proteins in shoots of *Salicornia europaea* under different salinity. *J. Proteome Res.* 8: 3331–3345.

Welti, R., Li, W., Li, M., Sang, Y., Biesiada, H., Zhou, H.-E., et al. (2002) Role of phospholipase D in freezing-induced lipid changes in Arabidopsis. *J. Biol. Chem.* 277: 31994–32002.

Wu, J., Seliskar, D.M. and Gallagher, J.L. (2005) The response of plasma membrane lipid composition in callus of the halophyte *Spartina patens* (Poaceae) to salinity stress. *Am. J. Bot.* 92: 852–858.

Yamaoka, Y., Yu, Y., Mizoi, J., Fujiki, Y., Saito, K., Nishijima, M., et al. (2011) *PHOSPHATIDYLSERINE SYNTHASE1* is required for microspore development in *Arabidopsis thaliana*. *Plant J.* 67: 648–661.

Yeung, T., Gilbert, G., Shi, J., Silvius, J., Kapus, A. and Grinstein, S. (2008) Membrane phosphatidylserine regulates surface charge and protein localization. *Science* 319: 210–213.

Yin, H., Gao, P., Liu, C., Yang, J., Liu, Z. and Luo, D. (2013) SUI-family genes encode phosphatidylserine synthases and regulate stem development in rice. *Planta* 237: 15–27.

Yu, Y., Kou, M., Gao, Z., Liu, Y., Xuan, Y., Liu, Y., et al. (2019) Involvement of phosphatidylserineand triacylglycerol in the response of sweet potato leaves to salt stress. *Front.Plant Sci* 10:1086.

Zhang, Z., Hui, E., Chapman, E. and Jackson, M.B. (2009) Phosphatidylserine regulation of Ca^{2+}-triggered exocytosis and fusion pores in PC12 cells. *Mol. Biol. Cell* 20: 5086–5095.

Zhu, J.K. (2003) Regulation of ion homeostasis under salt stress. *Curr. Opin. Plant Biol.* 6: 1–5.